32nd URSI GASS, Montreal, 19-26 August 2017

Compact cm-Wave and mm-Wave Integrated Receivers

Matthew A. Morgan*, Stephen D. Wunduke, Jason J. Castro, Tod A. Boyd, and Wavley Groves
National Radio Astronomy Observatory (NRAO), Charlottesville, VA, 22903, https://www.nrao.edu

Abstract

We will review the latest advances in compact, integrated analog-digital-photonic receivers for radio astronomy. Utilizing a number of novel architectural techniques, such as numerically calibrated digital sideband separation and polarization synthesis, amplitude- and phase-stabilizing reflectionless filters, and unformatted serial data links, these units are ideal for focal plane arrays and phased-array feeds (PAFs) at any frequency, as well as cost-efficient field-replaceable front-end modules on large-*N*/small-*D* interferometers. These techniques are illustrated in this summary paper via practical examples ranging from L-Band (1.2 – 1.7 GHz) to W-band (75 – 110 GHz).

1. Introduction

The purpose of the Integrated Receiver Development (IRD) program at the NRAO is to develop and optimize receiver architecture for the demands of future radio telescope facilities, such as the next-generation Very Large Array (ngVLA), the high-frequency Square Kilometer Array (SKA), and beyond. This is achieved via the close coordination of modern digital signal-processing (DSP) capabilities with state-of-the-art, integrated front-end design. The precision and fidelity of DSP post-processing, when carefully calibrated, is complementary to the very stable and uniform analog performance afforded by compact, integrated receiver design.

Specific aims of the IRD program include digitization of the information from the sky as early as possible in the signal path, and minimization of size, cost, and power dissipation per polarization channel. Not surprisingly, these goals often result in orthogonal design pressures that must be resolved in the context of particular application requirements – e.g., a single-dish phased-array feed or large-scale interferometer. Nonetheless, some general techniques have been developed to facilitate these optimizations, many of which have been reported in previous publications. The purpose of this paper is to show their unified application to complete, previously unpublished front-end receiver prototypes.

2. Novel Architectural Concepts

A simplified block diagram of a typical IRD front-end is shown in Figure 1 (this is meant to be a general illustration only, to facilitate the following discussion, as specific details will vary from one implementation to the next). A single polarization channel as shown is assumed to be driven by a cryogenic pre-amplification stage, connected to whatever feed structure is appropriate to the particular application. The integrated front-end module contains all the requisite warm post-amplification, downconversion, filtering, digitization, and laser transmission necessary to get the digital data stream away from the focal plane and off the telescope, on its way to a central signal processing facility (the back-end).

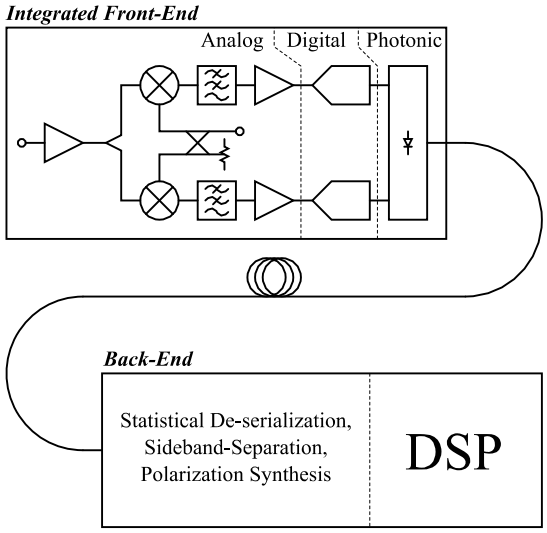

Figure 1. General block diagram of an integrated analog-digital-photonic front-end (single channel shown) with coordinated back-end processing algorithms.

In keeping with the stated goals of the IRD program, the front-end incorporates the minimum required electronics deemed necessary to capture the information from the sky with maximum fidelity. Any function which can feasibly be accomplished in the digital domain is deferred to the back-end, off the telescope. (Note that at the lowest RF frequencies, then, the front-end may not even include the downconversion stage shown, as the entire RF bandwidth could be digitized directly.)

2.1 Calibrated Digital Sideband-Separation

One of the weaknesses of integrated module construction using MMIC chips and surface-mount components (when compared to older sub-assemblies of connectorized parts) is the relatively poor isolation between signal paths. This

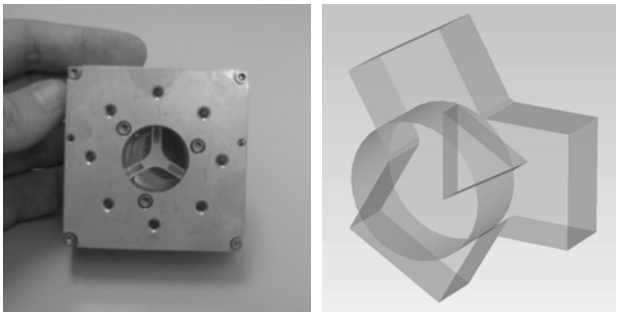

(a) (b)

Figure 2. (a) X-band (8-12 GHz) digitally-calibrated OMT [4]. (b) Simulation model of a 600-800 GHz digitally-calibrated OMT.

drives one to choose an architecture that minimizes the number of CW tones input into the receiver, to mitigate the risk of higher-order spurious mixing products.

For those receiver channels that cannot be digitized directly, then, we elect to use a single-stage, direct-to-baseband I/Q down-conversion, even from millimeter-wave frequency bands. The I and Q channels are individually digitized, and the amplitude and phase of the preceding (minimal) analog electronics is carefully calibrated so that the upper and lower sidebands can be reconstructed in the back-end with extraordinary precision. Experiments have shown that a well-designed integrated module can achieve image-rejection levels of 50 to 60 dB with calibrations that are stable over very wide temperature ranges and for virtually unlimited periods of time [1-4].

2.2 Calibrated Digital Polarization Synthesis

In a manner similar to the numerical sideband-separation described above, the IRD front-end can also incorporate a digital polarization synthesis function, whereby vector components of the incoming polarization-state are independently processed with signal paths like that shown in Figure 1, and re-combined in the back-end with calibrated coefficients to re-construct linear or circular polarizations, or the Stoke's parameters, as needed [5].

The benefits of this approach depend on the frequency band. At cm-wave frequencies (see Figure 2(a)), it enables the Orthomode Transducer (OMT) to be replaced by a compact module with simple field probes in the cold space, an order of magnitude smaller than waveguide assemblies with comparable performance. In some cases, it may also admit a common-mode input that is numerically orthogonal to the incoming sky polarizations, allowing a pilot tone or coherent noise to be injected for calibration purposes without masking the observation, and obviating the need for a separate calibration coupler which may add loss ahead of the cryogenic amplification.

At mm-wave and submm-wave frequencies, the intrinsic numerical calibration alleviates issues associated with manufacturing tolerances. The electromagnetic model for a three-way turnstile junction shown Figure 2(b) has no higher-order modes that can become trapped and resonant over the full waveguide bandwidth, and any imperfection in the geometry that leads to imbalance in the output arms is both stable and automatically calibrated out.

2.3 Reflectionless Filters

It is clear that the numerical methods above work best when the amplitude and phase characteristics of the analog signal path are as stable as possible. The integrated approach goes a long way to ensuring this calibration longevity, however early experiments revealed that in a compact module with gain suitable for radio astronomy, a very small residual instability existed that was ultimately traced to out-of-band signal energy becoming trapped between the mixers or amplifiers and the filters intended to limit the spectrum. This ultimately led to the invention of novel reflectionless filter topologies which absorb the unwanted stop-band, and enable an unprecedented level of amplitude and phase stability in our analog signal paths [6-11]. These filters have found widespread use in all areas of electronics and are now available commercially in die form or tiny surface-mount packages [12].

2.4 Unformatted Serial Data Links

In accordance with the goal of digitizing early, we are compelled to integrate the digital transmission of data away from the focal plane within the front-end module. If this were implemented using conventional methods, the digital overhead associated with packetizing and formatting the data stream would consume an unacceptable portion of the total power dissipated in the focal plane, while exacerbating the problem of filtering out self-generated radio-frequency interference (RFI).

To solve this problem, we developed a technique for the serial transfer of unformatted digital data, obtained directly from the sampler without further manipulation in the front-end. The technique leverages the known statistics of radio astronomy data streams, which is universally well-characterized by samples of Gaussian-distributed, white-noise [13-14].

3. Prototype Modules from 1 to 110 GHz

These ideas have been incorporated into a number of prototype front-ends that serve to illustrate how they all work together to create an optimized high-performance receiver.

3.1 L-band Phased-Array Feed Front-End

The first such module is a 40-channel warm-front end created for an L-Band (1.2-1.5 GHz) Phased-Array Feed [15], shown in Figure 3. Fed by a dipole array with cryogenic amplifiers, these warm modules provide the

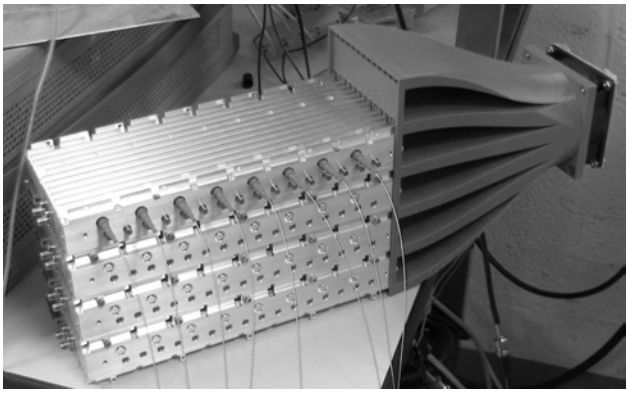

Figure 3. Partially-constructed 40-channel PAF front-end Four out of 5 blades shown, cooling plenum on the right.

remaining post-amplification, power levelling, down-conversion, filtering, digitization, and data transmission on optical fiber. After I/Q down-conversion, it samples the IF signal at baseband with 8-bit resolution, and provides 155 MHz of instantaneous bandwidth (upper and lower sidebands combined) for all 40 channels simultaneously. The output is carried on individual single-mode fibers operating at 1310 nm and 2.5 Gbps. The entire array is built as a stack of 5 *blades* incorporating 8 channels each, and measures about 10 x 18 x 24 cm.

3.2 S-Band Research Prototype

Another prototype was constructed at S-band (1.7-2.6 GHz) to demonstrate operation of the unformatted serial link at lower bit-resolutions — which slightly modifies the statistics depended upon for de-serialization, described earlier. Sampling at only 4 bits, but using the same 2.5 Gbps fiber link rate, this module provides 622 MHz of instantaneous bandwidth. This was considered a step toward higher bandwidth as well as higher RF frequency where, in radio astronomy, lower bit-resolutions are commonly preferred. Smaller than a typical smartphone, this module, shown in Figure 4, incorporates all the functions of a complete radio astronomy receiver channel and delivers its output on single-mode fiber with up to 5 km reach.

3.3 W-band Research Prototype

Having successfully demonstrated the techniques described here in multiple cm-wave frequency bands, our current efforts are focused on scaling them up to mm-wave frequencies. A new front-end prototype is now in the final design phase which will operate at input frequencies in W-Band (75-110 GHz) and provide 1 GHz of instantaneous bandwidth at 8 bit resolution.

The data-transmission elements of all the aforementioned front-ends have been built using off-the-shelf surface-mount ADCs and Serializers operating at 2.5 Gbps, however these components are not readily found for operation at higher speeds, except where integrated inside

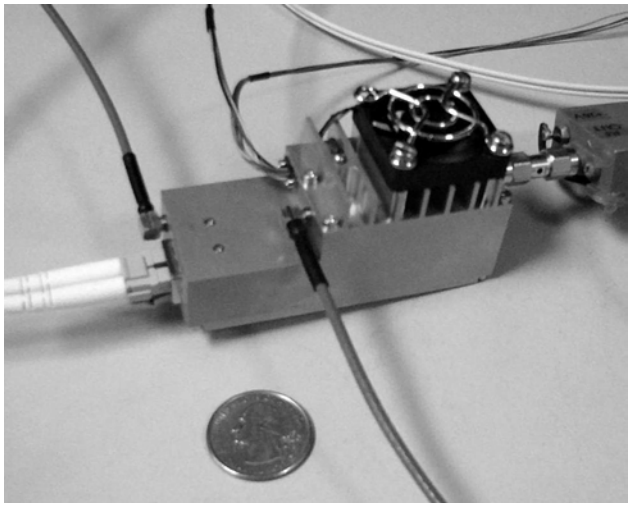

Figure 4. S-band (1.7-2.6 GHz) front-end prototype. An American quarter is shown for scale.

powerful (and power-hungry) computational platforms such as FPGAs. This is not compatible with the low-power, minimum-overhead paradigm of the IRD front-end program. The eventual aim of this program is to make a resolution-agnostic ADC & Serializer as a unified ASIC to implement these functions. Initial estimates promise an order of magnitude reduction in power dissipation and footprint. Unfortunately, the funding for such a development has not yet materialized.

As a result, the W-band prototype of this section is being designed to use a single FPGA as the serializing element for multiple channels. While it will undoubtedly consume much more power than the equivalent module using an ASIC, it is deemed an acceptable compromise for proving the concept at higher RF frequencies and bandwidths.

The module will deliver digitized I and Q outputs from each of two polarization channels on a QSFP output — that is, on a single fiber using four light wavelengths, each modulated at 8 Gbps. The receive channel of the QSFP output will essentially be dormant, but could be used for M&C or to cross-connect modules for some pre-processing of the data, such as beamforming in a phased array.

An exploded mechanical view of the W-Band module under development is shown in Figure 5.

4. Acknowledgements

This work was funded by the Integrated Receiver Development program at the National Radio Astronomy Observatory. The National Radio Astronomy Observatory is a facility of the National Science Foundation operated under cooperative agreement by Associated Universities, Inc.

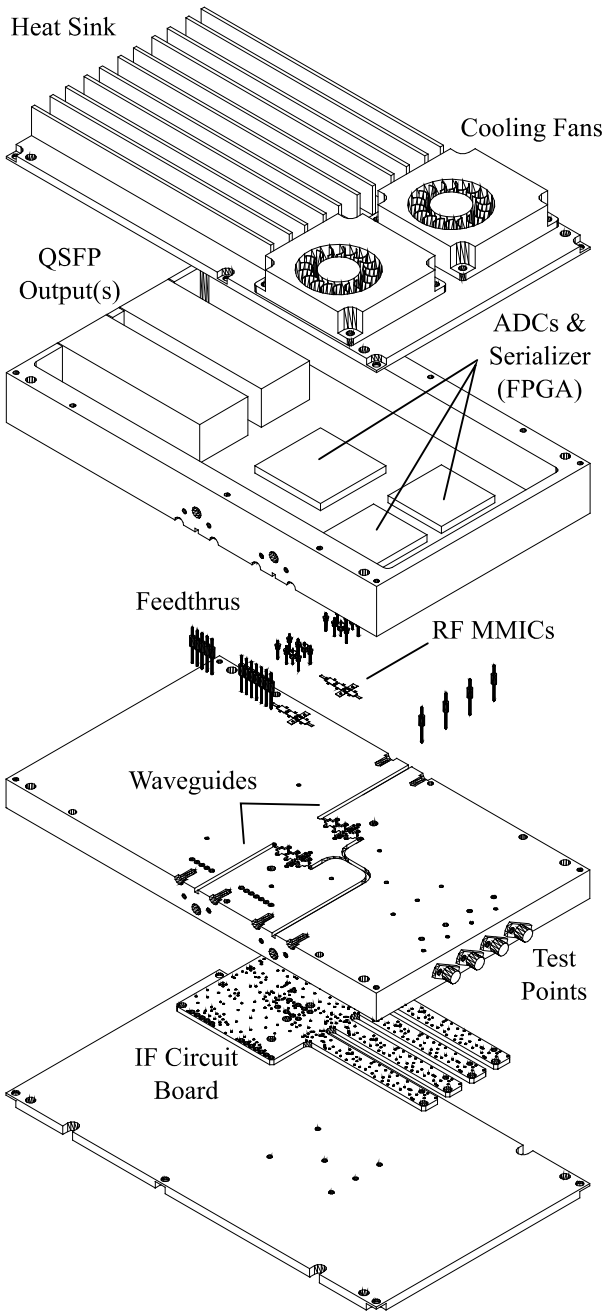

Figure 5. An exploded mechanical view of the W-band prototype front-end module.

5. References

1. M. Morgan and J. Richard Fisher, "Experiments With Digital Sideband-Separating Downconversion," *Publications of the Astronomical Society of the Pacific*, vol. 122, no. 889, pp. 326-335, March 2010.

2. R. Finger, P. Mena, N. Reyes, R. Rodriguez, and L. Bronfman, "A calibrated digital sideband separating spectrometer for radio astronomy applications," *Publications of the Astronomical Society of the Pacific*, vol. 125, no. 925, pp. 263-269, March 2013.

3. R. Finger, F. P. Mena, A. Baryshev, A. Khudchenko, R. Rodriguez, E. Huaracan, A. Alvear, J. Barkhof, R. Hesper, and L. Bronfman, "Ultra-pure digital sideband separation at sub-millimeter wavelengths," *Astronomy and Astrophysics*, vol. 584, December 2015.

4. J. Castro, M. Morgan, J. Ford, and V. van Tonder, "Digital sideband separating downconversion for the Green Bank Telescope phased array feed," *URSI National Radio Science Mtg.*, Boulder, CO, January 2016.

5. M. Morgan, J. Fisher, and T. Boyd, "Compact Orthomode Transducers Using Digital Polarization Synthesis," *IEEE Trans. Microwave Theory Tech.*, vol. 58, no. 12, pp. 3666-3676, December 2010.

6. M. Morgan and T. Boyd, "Theoretical and Experimental Study of a New Class of Reflectionless Filter," *IEEE Trans. Microwave Theory Tech.*, vol. 59, no. 5, pp. 1214-1221, May 2011.

7. M. Morgan and T. Boyd, "Reflectionless Filter Structures," *IEEE Trans. Microw. Theory Techn.*, vol. 63, no. 4, pp. 1263-1271, April 2015.

8. M. Morgan, "Reflectionless Filters," *U.S. Patent No. 8,392,495*, March 5, 2013. *People's Republic of China Patent No. 201080014266.1*, July 30, 2014.

9. M. Morgan, "Transmission Line Reflectionless Filters," *U.S. Patent Application No. 14/927,881*, October 30, 2015.

10. M. Morgan, "Sub-Network Enhanced Reflectionless Filter Topology," *U.S. Patent Application No. 14/724,976*, May 29, 2015.

11. M. Morgan, *Reflectionless Filters*, Norwood, MA: Artech House, January 2017.

12. X-Series filters, http://www.minicircuits.com

13. M. Morgan, J. Fisher, and J. Castro, "Unformatted Digital Fiber-Optic Data Transmission for Radio Astronomy Front Ends," *Publications of the Astronomical Society of the Pacific*, vol. 125, no. 928, pp. 695-704, June 2013.

14. M. Morgan and J. Fisher, "Statistical Word Boundary Detection in Serialized Data Streams," *U.S. Patent No. 8,688,617*, April 1, 2014.

15. A. Roshi, K. Warnick, J. Brandt, J. Fisher, B. Jeffs, P. Marganian, M. McLeod, M. Morgan, M. Mello, R. Norrod, W. Shillue, R. Simon, and S. White, "A 19 element cryogenic phased array feed for the Green Bank telescope," *IEEE Intl. Symp. Antennas and Propagation and URSI CNC/USNC Joint Mtg.*, Vancouver, BC., Canada, July 19-25, 2015.